Received: 4 December 2017 | Revised: 4 February 2018 | Accepted: 11 February 2018

DOI: 10.1002/aoc.4344

FULL PAPER

WILEY Applied Organometallic Chemistry

Novel design of recyclable copper(II) complex supported on magnetic nanoparticles as active catalyst for Beckmann rearrangement in poly(ethylene glycol)

Mahdi Keyhaniyan | Ali Shiri | Hossein Eshghi | Amir Khojastehnezhad

Department of Chemistry, Faculty of Science, Ferdowsi University of Mashhad, Mashhad, Iran

Correspondence
Ali Shiri, Department of Chemistry, Faculty of Science, Ferdowsi University of Mashhad, Mashhad, Iran.
Email: alishiri@um.ac.ir

Funding information
Ferdowsi University of Mashhad Research Council, Grant/Award Number: 3/41331

Copper complex-functionalized magnetic core–shell nanoparticles (Fe_3O_4@SiO_2-Lig-Cu) were prepared and characterized using various techniques. The activity of the new catalyst was tested for the Beckmann rearrangement. The reaction conditions allow for the conversion of a wide variety of aldoximes, including aromatic and heterocyclic ones, to amides in good to excellent yields. High efficiency, mild reaction conditions, easy work-up, use of poly(ethylene glycol) as a green medium and simple purification of products are important advantages of this system. Moreover, the eco-friendly heterogeneous nanocatalyst could be easily recovered from the reaction mixture using an external magnet and reused several times.

KEYWORDS
aldoximes, amides, Beckmann rearrangement, Fe_3O_4@SiO_2-Lig-Cu, magnetic core–shell nanoparticles

1 | INTRODUCTION

Today, in the chemical industry, there is a growing need for green and more sustainable processes. As is well documented, use of catalytic reactants is a better choice than strategies in which stoichiometric reagents are used. Homogeneous catalysis approaches, due to uniform and well-defined reactive centres of the catalysts, facilitate mixing of the catalyst with the reaction mixture and attracted as much attention as heterogeneous ones. However, there are some problems like the cost and toxicity associated with metals used as catalysts in homogeneous methods, together with the loss of catalyst after one run.[1] To compensate for the deficiencies related to homogeneous catalysts, much efforts have been applied to combine the advantages of homogeneous and heterogeneous catalysis.[2,3] In this respect, metal nanoparticles have appeared and have been widely used in biomedicine, electronic devices, spectroscopy and especially in catalytic systems.[4] Although these nanoparticles with their large surface area show high catalytic activity in various types of organic reactions, there are two major drawbacks. First, easy aggregation of these nanoparticles with high surface energy deactivates the catalyst. Second, the small size of metal nanoparticles results in difficulty in separation and recovery from a reaction mixture.[5] In order to solve these issues, utilization of a catalyst support on which to load the metal nanoparticles has emerged. Recently, magnetic supports have been considered as the best choice duo to their eliminating the requirement of catalyst filtration and centrifugation. Facile isolation of catalyst from reaction mixture through a simple magnetic decantation is the main advantage of magnetic nanoparticle (MNP)-supported catalysts.[6]

The amide bond is considered as one of the most important linkages in organic chemistry. Moreover, in biological chemistry, the formation of amide bonds is argued as the most important chemical transformation owing to the widespread appearance of amides in pharmaceuticals, natural products and peptides.[7] Amides in conjugation with other aliphatic, aromatic and heterocyclic rings

produce various types of biological activity. They possess a wide spectrum of biological activities like antituberculosis, anticonvulsant, analgesic, anti-inflammatory, insecticidal, antifungal and antitumour properties.[8–12]

In the conventional approach, amides are synthesized by coupling of carboxylic acids and amines in the presence of a stoichiometric coupling agent or application of activated carboxylic acid derivatives which is not desirable due to low atom economy.[13,14] The metal-catalysed rearrangement of aldoximes has emerged in recent years as a promising strategy to achieve amide transformations.[15] In recent decades several catalysts such as CuO–ZnO/C,[16] Au/TiO_2,[17] $[Pd(cinnamyl)Cl]_2$,[18] bis(allyl)–ruthenium(IV),[19] $[RuCl_2(\eta^6\text{-}p\text{-cymene})]$,[20] $[RuCl_2(\eta^6\text{-}C_6Me_6)\{P(NMe_2)_3\}]$,[21] $CuSO_4{\cdot}5H_2O$,[22] $\{Co^{III}–Zn^{II}\}$ heterometallic complexes,[23] $KMnO_4/NH_{3(l)}$,[24] $Al_2O_3/MeSO_2Cl$,[25] $ZnCl_2/K_2CO_3$,[26] $RuCl(PPh_3)_3$,[27] Cu_2O,[28] $CuCl_2$,[29] Cs_2CO_3,[30] ZnO,[31] SBA-15/En–Cu[32] and *Rhodococcus rhodochrous* cells[33] have been used for primary amide preparation from aldoximes. Despite the development of these reported procedures for conversion of aldoximes to amides, there are still limitations in some respects, including harsh reaction conditions, specially prolonged reaction times, use of microwave power and high temperature, lack of generality and use of high-cost or less readily available reagents. So, in order to overcome these drawbacks, we wanted to identify a heterogeneous catalyst for use under green conditions, which was cheap, effective at lower catalyst loading in short reaction time and could be used under milder conditions than those previously reported.

Inspired by the above discussion and considering green and sustainable chemistry, it is highly desirable to develop a new catalytic system for use under mild conditions, with low catalyst loading and involving relatively cheap metals. Therefore, in the work reported here, we designed and prepared a novel magnetic nanocatalyst (Fe_3O_4@SiO_2-Lig-Cu) as illustrated in Scheme 1. The catalytic activity of the prepared nanocatalyst was investigated in the transformation of aldoximes to amides in poly(ethylene glycol) (PEG) as a green medium at 80 °C (Scheme 2).

2 | RESULTS AND DISCUSSION

2.1 | Preparation and Characterization of Catalyst

At first, Fe_3O_4 MNPs were prepared by a chemical co-precipitation method using $FeCl_2{\cdot}4H_2O$ and $FeCl_3{\cdot}6H_2O$ as precursors.[34] In the next step, the prepared nanoparticles were easily coated with a layer of SiO_2 in a mixture of aqueous ammonia, tetraethylorthosilicate (TEOS) and ethanol via a sol–gel method to afford Fe_3O_4@SiO_2 MNPs. These MNPs were allowed to react with (3-aminopropyl) triethoxysilane and then with 3-chloropropane-1,2-diol to give Fe_3O_4@SiO_2-Lig MNPs. Finally, copper(II) acetate was grafted on the modified Fe_3O_4@SiO_2 MNPs leading to Fe_3O_4@SiO_2-Lig-Cu (Scheme 1). The prepared catalyst was characterized using various techniques including Fourier transform infrared (FT-IR) spectroscopy, X-ray diffraction (XRD), scanning electron microscopy (SEM), transmission electron microscopy (TEM), energy-dispersive X-ray (EDX) analysis, thermogravimetric analysis (TGA), vibrating sample magnetometry (VSM) and inductively coupled plasma (ICP) anlysis.

The FT-IR spectra of Fe_3O_4, Fe_3O_4@SiO_2, Fe_3O_4@SiO_2-NH_2, Fe_3O_4@SiO_2-Lig, fresh Fe_3O_4@SiO_2-Lig-Cu and reused Fe_3O_4@SiO_2-Lig-Cu are compared in

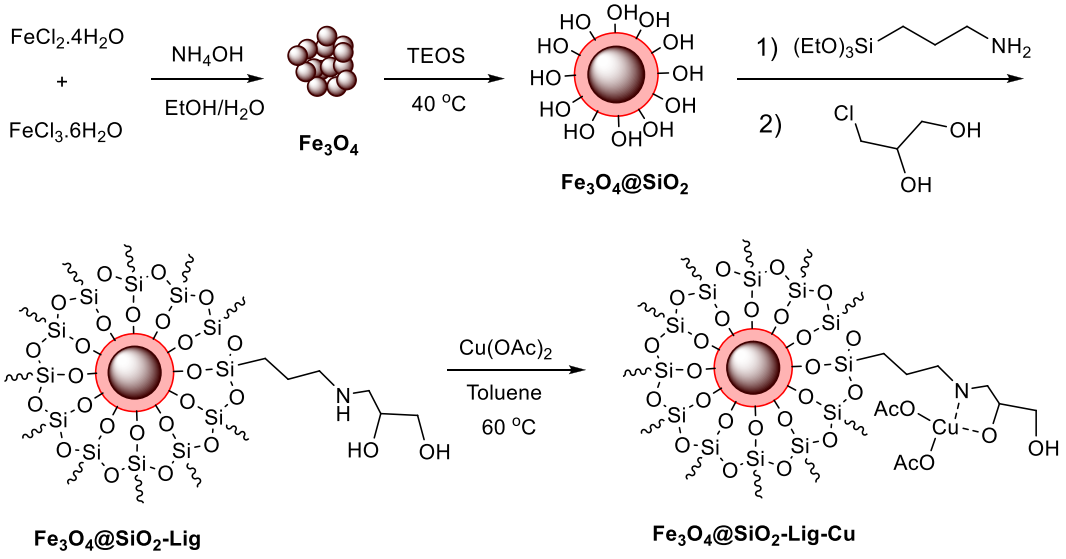

SCHEME 1 Preparation of magnetic nanocatalyst (Fe_3O_4@SiO_2-Lig-Cu)

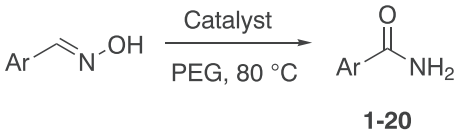

SCHEME 2 Synthesis of amide derivatives via Beckmann rearrangement in presence of Fe_3O_4@SiO_2-Lig-Cu

Figure 1. A strong band at around 465–563 cm^{-1} appeared in the spectra of all the MNPs which can be assigned to the stretching vibration of Fe—O bond. The broad characteristic band at 3420 cm^{-1} is related to O—H stretching vibration, demonstrating the presence of hydroxyl groups on the surface of Fe_3O_4 MNPs.[35] In comparison with Figure 1(a), in Figure 1(b), the intensity of the band of the Fe—O bond significantly weakens and a strong absorption peak at 1096 cm^{-1} and weak absorption peak at 943 cm^{-1} appeared attributed to asymmetric vibration of the Si—O—Si bond and the symmetric stretching of the Si—OH bond, respectively. For Fe_3O_4@SiO_2-NH_2 (Figure 1c), 3-aminopropyltriethoxysilane was grafted to the Fe_3O_4@SiO_2 framework, which was recognized by the methylene C—H stretching and —NH bending vibration bands at 2925 and 1646 cm^{-1}.[36] Appearance of a broad absorption band at around 3000–3600 cm^{-1} attributed to —OH and —NH stretching frequencies and, furthermore, an increase of the intensity of C—H stretching vibration confirm the successful reaction between 3-chloro-1,2-propanediol and Fe_3O_4@SiO_2-NH_2 (Figure 1d). The FT-IR spectrum of fresh Fe_3O_4@SiO_2-Lig-Cu is the same as previous spectra (Figure 1e). Unfortunately, the absorption bands related to coordination of Cu(II) with nitrogen and oxygen were covered by stretching vibration frequencies of Fe—O and Si—O bonds.[37] For solving this issue, a new expanded FT-IR spectrum of Figure 1(e) was studied (Figure 2). The absorption bands at 428 and 450 cm^{-1} confirm the successful immobilization of Cu with nitrogen (Cu—N) and oxygen (Cu—O) groups. Finally, The FT-IR spectrum of reused catalyst (Figure 1f) shows that the structure of the catalyst remains almost the same after five recycles.

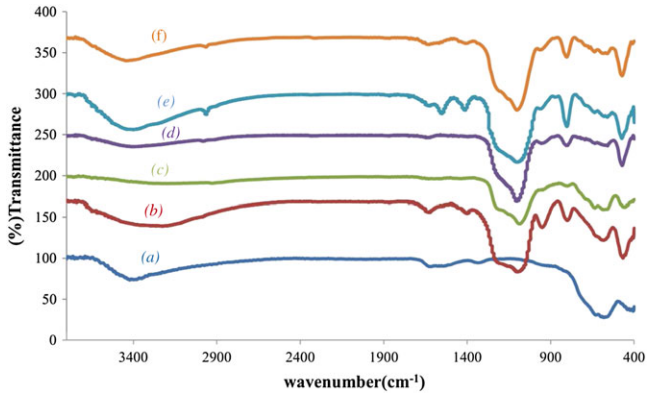

FIGURE 1 FT-IR spectra of (a) Fe_3O_4 MNPs, (b) Fe_3O_4@SiO_2 MNPs, (c) Fe_3O_4@SiO_2-NH_2 MNPs, (d) Fe_3O_4@SiO_2-Lig, (e) fresh Fe_3O_4@SiO_2-Lig-Cu MNPs and (f) Fe_3O_4@SiO_2-Lig-Cu MNPs after five cycles

The morphological features were studied using the SEM technique. The SEM image of Fe_3O_4@SiO_2-Lig-Cu (Figure 3) demonstrates that the MNPs are almost spherical, narrowly distributed and well dispersed. Also, the particle size of the nanocatalyst was investigated using the TEM technique (Figure 4). The TEM image of the sample shows the average size of Fe_3O_4@SiO_2-Lig-Cu magnetic nanocatalyst particles is between approximately 20 and 25 nm in diameter.

The signal of Cu element along with other elements including Fe, Si, O and C in the EDX spectrum of the

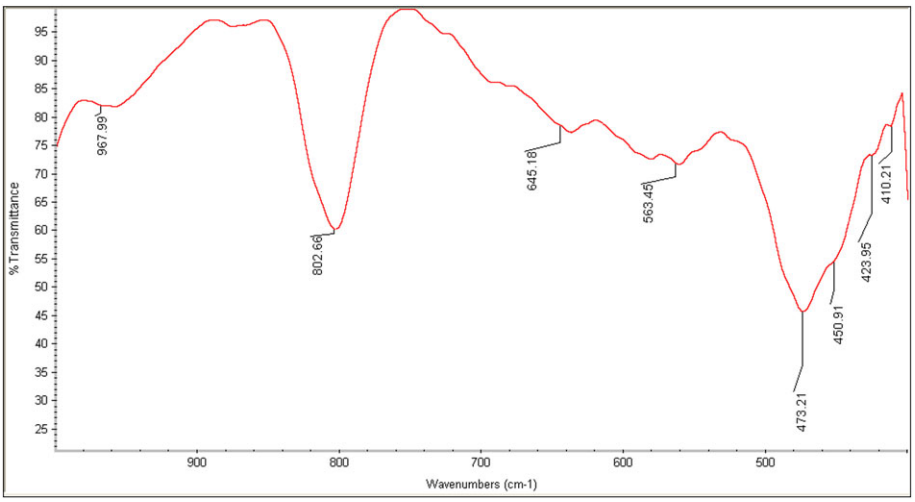

FIGURE 2 Expanded FT-IR spectrum of Fe_3O_4@SiO_2-Lig-Cu MNPs between 400 and 1000 cm^{-1}

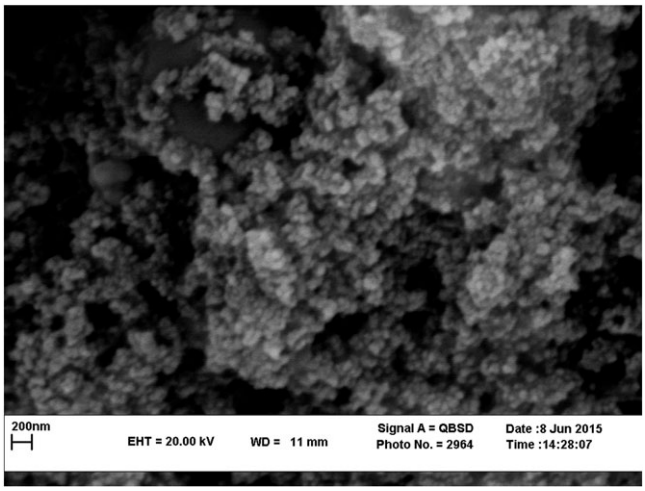

FIGURE 3 SEM image of Fe_3O_4@SiO_2-Lig-Cu

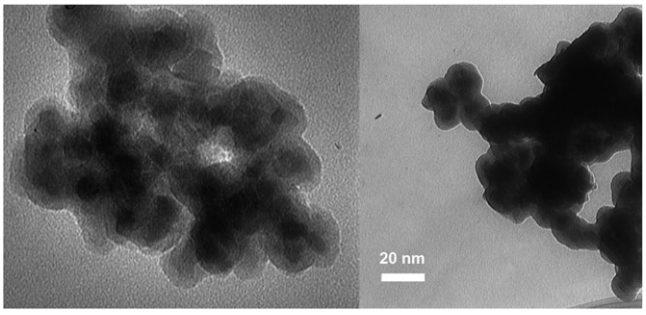

FIGURE 4 TEM images of Fe_3O_4@SiO_2-Lig-Cu

Fe_3O_4@SiO_2-Lig-Cu catalyst shows the successful immobilization of Cu(II) acetate and organic compounds on Fe_3O_4@SiO_2 MNPs. As can be seen in Figure 5, no additional peak related to other impurities appeared in the spectrum, except for Al that corresponds to aluminium stubs and Au related to the gold sputtering technique for EDX. Samples were processed for SEM–EDX analysis by mounting the drop-exposed, fixed specimens on aluminium stubs. The specimens then were overcoated with sputtered gold.[38]

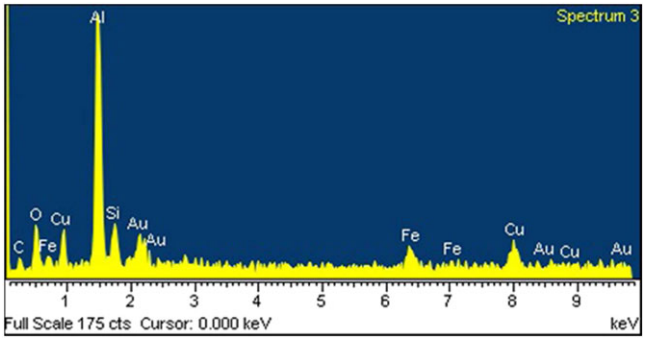

FIGURE 5 EDX pattern of Fe_3O_4@SiO_2-Lig-Cu

XRD analysis was applied to identify the crystalline structure of Fe_3O_4@SiO_2-Lig-Cu. As indicated in Figure 6, six diffraction peaks at $2\theta = 30.31°$, 35.64°, 43.31°, 53.86°, 57.24° and 62.83° are attributed to the (220), (311), (400), (422), (511) and (440) crystal planes of magnetite (Fe_3O_4)[39] with cubic phase according to JCPDS card no. 19–0629 (Figure 6a) which indicates the pure crystalline structure of magnetite. As shown in Figure 6(b), the XRD pattern of Fe_3O_4@SiO_2-Lig-Cu shows a broad peak at $2\theta = 23°$ which is attributed to the amorphous silica shell,[40] in addition to the six diffraction peaks of Fe_3O_4 MNPs. No marked changes occur in the number of peaks, but due to the silica coating, the characteristic peaks of Fe_3O_4 become weak in Figure 6 (b). The average crystallite size of Fe_3O_4 MNPs calculated using the Debye–Scherrer equation ($d = K\lambda/\beta\cos\theta$) is about 23 nm on (311) crystal plan. These results indicate that the crystal structure of Fe_3O_4 core remains unchanged after coating with silica shell. The peaks related to Cu(II) acetate appeared between $2\theta = 10°$ and 25°, but because of the overlap with broad silica peak in these regions, the characterization of mentioned peaks is impossible.[41,42] Moreover, the XRD pattern of reused catalyst after five runs is shown in Figure 6(c) that confirms the structure of the catalyst remains almost the same after five runs.

TGA was used to confirm the high thermal stability of the Fe_3O_4@SiO_2-lig-Cu catalyst. As we can see in Figure 7, there are two main weight losses. Firstly, the weight loss (4%) at around 100–380 °C is allocated to physically and hydrogen bonded water on the support. The second weight loss (6%) in the range 400–550 °C is related to the organic parts which are anchored to the Fe_3O_4@SiO_2 surface. Based on the TGA analysis results, ligand grafting had been successfully accomplished.

It is of great importance that the core–shell material should possess sufficient magnetic and superparamagnetic properties for its practical application.

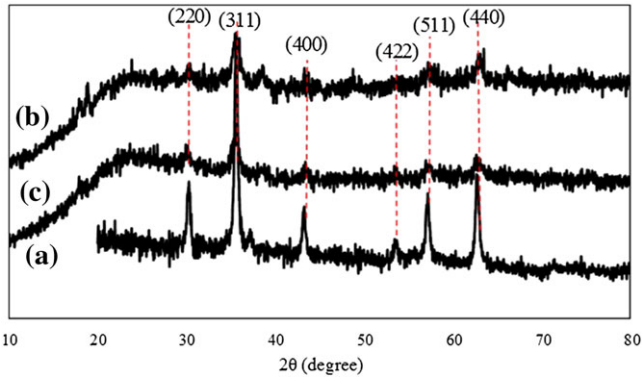

FIGURE 6 XRD patterns of (a) standard Fe_3O_4, (b) fresh Fe_3O_4@SiO_2-Lig-Cu MNPs and (c) reused Fe_3O_4@SiO_2-Lig-Cu

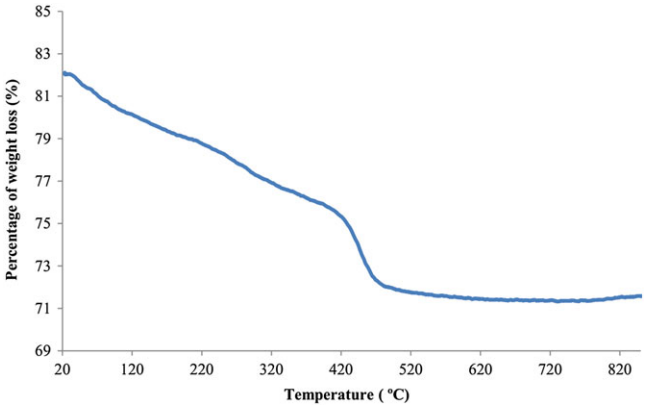

FIGURE 7 TGA curve of Fe_3O_4@SiO_2-Lig-Cu MNPs

Magnetic hysteresis measurements for the catalyst were done in an applied magnetic field at room temperature, with the field sweeping from −15 000 to +15 000 Oe. As shown in Figure 8, the *M*(*H*) hysteresis loop for the samples was completely reversible, showing that the MNPs exhibit superparamagnetic characteristics. The hysteresis loops reached saturation up to the maximum applied magnetic field. The magnetic saturation value of the sample is 12 emu g^{-1} at room temperature. These MNPs showed high permeability in magnetization and their magnetization was sufficient for magnetic separation with a conventional magnet.

Finally, the copper content of the prepared Fe_3O_4@SiO_2-Lig-Cu was determined using ICP analysis. According to this, the amount of copper in the catalyst is 2.05 mmol g^{-1}. This result shows the good immobilization of Cu(II) on Fe_3O_4@SiO_2-Lig MNPs.

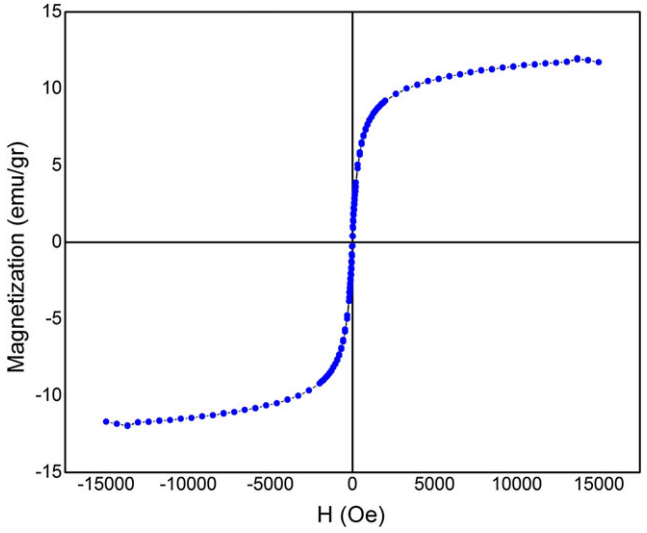

FIGURE 8 Magnetization curve of Fe_3O_4@SiO_2-Lig-Cu

2.2 | Catalytic Application of Fe_3O_4@SiO_2-Lig-Cu

Catalytic activity of the synthesized magnetic nanocatalyst was investigated in order to prepare aromatic and heteroaromatic amides through Beckmann rearrangement. To achieve the maximum yield and efficiency for preparation of amides, experimental conditions must be carefully optimized. For this purpose, conversion of 4-methylbenzaldoxime to 4-methylbenzamide was selected as a model reaction. Initially, the influences of solvent and catalyst were investigated, and the results are summarized in Table 1. As can be seen, no progress in the reaction was observed in the absence of catalyst even after 24 h (entry 1). Employing toluene, ethanol and water as solvents led to moderate yields in the presence of the nanocatalyst (entries 5, 6 and 8). Compared with those solvents, higher yields of 70 and 65% were observed when dimethylformamide (DMF) and CH_3CN were adopted (entries 9 and 10). Surprisingly, the progress of reaction was observed in a satisfactory time with PEG as a green solvent (entry 11).

After that the effects of catalyst loading and temperature were examined. Increasing the catalyst loading from 3 to 5 mol% led to enhanced efficiency (entries 13 and 14). On the other hand, a yield of only 30% was achieved by reducing the catalyst loading to 2 mol% (entry 12). Conducting the reaction at 60 °C reduced the reaction yield and elevated temperature of 100 °C also led to decreased yield (entries 16 and 17). So, the best result in terms of yield as well as reaction time was observed in PEG at 80 °C with 4 mol% of catalyst (entry 14). This reaction was also carried out in presence of copper acetate ($Cu(OAc)_2$). In comparison to the prepared catalyst, the homogeneous copper acetate was not efficient for this reaction and the yield of the reaction was only 80% after 180 min (entry 18).

Encouraged by the optimization results, a broad range of differently substituted aromatic aldoximes were investigated for amide bond formation (Table 2). Various aromatic aldoximes bearing electron-donating substituents such as a methoxy group (entry 12) as well as electron-withdrawing nitro group (entry 6) were applied in this transformation to afford the corresponding products **1**–**20** in good to excellent yields. Moreover, α,β-unsaturated cinnamaldoxime as a suitable substrate was applied successfully to obtain the desired product in 87% yield (entry 16). To our disappointment, *ortho*-methoxy-substituted aldoxime only provided low yield of product; however, a high yield of 89% was achieved for *ortho*-chloro-substituted aldoxime into primary amide **8**. Meanwhile, moderate transformation was observed for 2-hydroxy-substituted aldoxime, which generated

TABLE 1 Optimization of amount of Fe_3O_4@SiO_2-Lig-Cu nanocatalyst and effect of solvent and temperature for preparation of 4-methylbenzamide (**3**)[a]

Entry	Catalyst (mol%)	Solvent (1 ml)	Temp. (°C)	Time (h)	Yield (%)
1	—	Solvent-free	r.t.	24	0
2	4	Solvent-free	80	24	0
3	4	CH_2Cl_2	r.t.	24	0
4	4	CH_2Cl_2	Reflux	24	0
5	4	Toluene	Reflux	24	50
6	4	EtOH	Reflux	24	45
7	4	Glycerol	80	24	20
8	4	H_2O	Reflux	24	50
9	4	DMF	80	24	70
10	4	CH_3CN	Reflux	24	65
11	4	PEG	80	5	72
12	2	PEG	80	5	30
13	3	PEG	80	5	65
14	**4**	**PEG**[b]	**80**	**1**	**85**
15	5	PEG[b]	80	1	85
16	4	PEG[b]	60	5	45
17	4	PEG[b]	100	5	62
18[c]	4	PEG	80	3	80

[a]Reaction conditions: 4-methylbenzaldoxime (1 mmol), $Cu(OAC)_2$ (4 mol%) and PEG.

[b]PEG (0.5 ml) was used.

[c]$Cu(OAC)_2$ was applied as a catalyst.

corresponding amide **18** in 60% yield. It is noteworthy that this catalytic system was also applied for heteroaromatic substrates such as those with pyridyl, thienyl and furanyl moieties. Surprisingly, for all heteroaromatic aldoximes, excellent yield of desired amides was achieved (entries 14, 19 and 20).

The reactivity of some selected aldoximes in Beckmann rearrangement in the same reaction time (60 min) was investigated (Table 3). We selected aldoximes bearing both electron-donating and electron-withdrawing substituents in *ortho*, *meta* and *para* positions (entries 1–8) as well as some aromatic and heteroaromatic systems (entries 9 and 10). Similar to results in Table 1, aldoximes with electron-withdrawing substituents (entries 2, 5 and 6) give higher yields compared to those with electron-donating groups (entries 3 and 4). Also, the heteroaromatic furyl system (entry 10) afforded better yield, while a bulky system like naphthyl gave a low yield (entry 9).

The possibility of recycling and reusing the Fe_3O_4@SiO_2-Lig-Cu MNPs was examined using the same model reaction under the aforementioned optimized reaction conditions (Figure 9). Upon completion of the first run, the magnetic nanocatalyst was separated from the reaction mixture using an external magnet, washed with water and ethanol, dried at 80 °C overnight and then used in the next run. The catalyst could be used at least five times with only a slight reduction in activity, which clearly demonstrates the practical reusability of this catalyst.

A plausible mechanism for the conversion of aldoxime to amide in the presence of Cu-immobilized modified Fe_3O_4 MNPs has been studied (Scheme 3). This involves activation of aldoxime with Cu(II) Lewis acid followed by dehydration and then formation of five-membered cyclic intermediate, which leads to the final amide product.

3 | EXPERIMENTAL

3.1 | Chemicals and Apparatus

Melting points of products were recorded with an Electrothermal type 9200 melting point apparatus. FT-IR spectra were recorded with a Nicolet Avatar 370 FT-IR spectrometer. NMR spectra were obtained with a Bruker AC instrument at 300 MHz in DMSO-d_6. Mass spectra were obtained with a Varian Mat CH-7 at 70 eV. The crystal

TABLE 2 Conversion of oximes into amides (**1**–**20**) using Fe_3O_4@SiO_2-Lig-Cu nanocatalyst[a]

Entry	Ar	Time (h)	Yield (%)	M.p. (°C)
1	C_6H_5	1	87	126–127[16]
2	4-BrC_6H_4	1	90	189–191[17]
3	4-MeC_6H_4	1	85	154–156[16]
4	4-iso-PrC_6H_4	1	93	152–154[18]
5	3-MeC_6H_4	1	85	88–90[19]
6	4-$NO_2C_6H_4$	1	92	199–200[20]
7	3-BrC_6H_4	1	90	157–159[21]
8	2-ClC_6H_4	1	89	135–137[22]
9	4-ClC_6H_4	1	95	170–172[23]
10	4-CNC_6H_4	1	80	222–224[24]
11	3-OHC_6H_4	1	93	170–171[25]
12	4-$OMeC_6H_4$	2	70	163–165[16]
13	3,4-$(Cl)_2C_6H_3$	3	90	138–139[26]
14	4-Pyridyl	1.5	95	155–157[27]
15	2-Naphthyl	3	75	196–198[28]
16	$C_6H_5CH{=}CH$	1	87	145–147[29]
17	2-OH,5-BrC_6H_3	3	67	236–238[30]
18	2-OH	3	60	138–140[31]
19	2-Thiophenyl	2	98	182–184[32]
20	2-Furyl	2	98	140–142[33]

[a]Reaction conditions: aldoxime (1 mmol), catalyst (4 mol%), PEG (0.5 ml) at 80 °C.

structure of the catalyst was analysed using XRD with a Bruker D8 ADVANCE diffractometer using a Cu target (λ = 1.54 Å). The magnetic property of the catalyst was measured using VSM (model 7400, Lake Shore). TEM

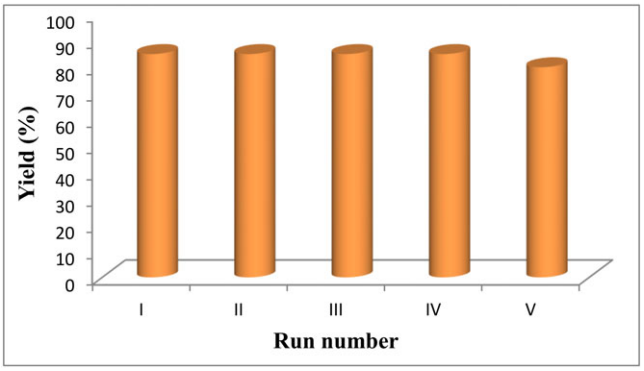

FIGURE 9 Recyclability of catalyst for preparation of 4-methylbenzamide (**3**)

was performed with a Leo 912AB (120 kV) microscope (Zeiss, Germany). ICP analysis was carried out with a Varian VISTA-PRO, CCD (Australia). Elemental compositions were determined with EDX analysis (model 7353, Oxford Instruments, UK), with 133 eV resolution. TGA was performed with a Shimadzu thermogravimetric analyser (TG-50) under air atmosphere at a heating rate of 10 °C min^{-1}.

3.2 | Preparation of Fe_3O_4@SiO_2 Core–Shell

Hydrolysis of TEOS in basic solution via the Stober method was applied to prepare core–shell Fe_3O_4@SiO_2 nanospheres.[43] An amount of 0.10 g of freshly prepared iron oxide was dispersed in 40 ml of ethanol (98%) and 10 ml of deionized water for 30 min. Then 1.5 ml of ammonia (25 wt%) was added and the resulting mixture was stirred at 40 °C for 30 min and TEOS (2.0 ml) was added and stirring was continued for 24 h at 40 °C. The

TABLE 3 Conversion of oximes into selected amides using Fe_3O_4@SiO_2-Lig-Cu nanocatalyst in the same reaction time[a]

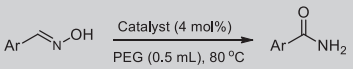

Entry	Ar	Time (h)	Yield (%)
1	C_6H_5	1	87
2	4-ClC_6H_4	1	95
3	4-$OMeC_6H_4$	1	55
4	2-OHC_6H_4	1	40
5	4-$NO_2C_6H_4$	1	92
6	4-CNC_6H_4	1	80
7	3-OHC_6H_4	1	92
8	2-OH,5-BrC_6H_3	1	38
9	2-Naphthyl	1	58
10	2-Furyl	1	88

[a]Reaction conditions: aldoxime (1 mmol), catalyst (4 mol%), PEG (0.5 ml) at 80 °C.

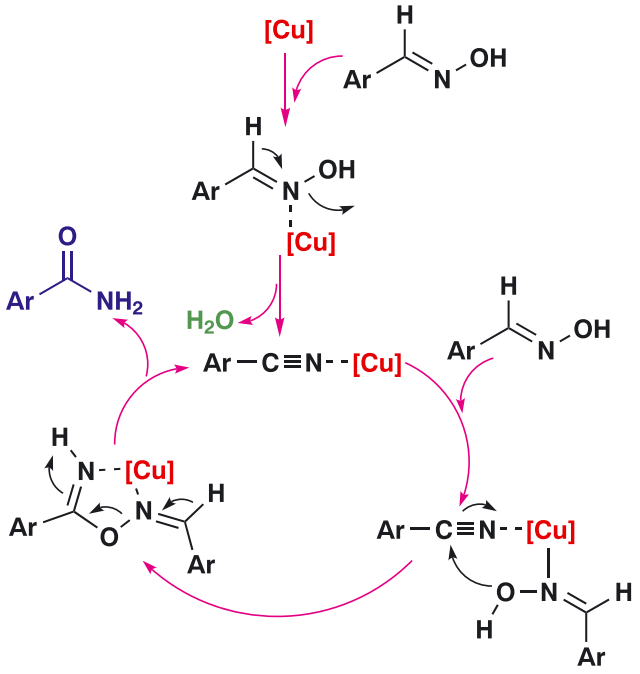

SCHEME 3 Proposed mechanism for synthesis of amide derivatives

obtained silica-coated MNPs were collected using a permanent magnet and washed three times with water and ethanol, and dried at 60 °C for 6 h.

3.3 | Preparation of Amino-Functionalized Fe_3O_4@SiO_2

According to the literature,[44] prepared Fe_3O_4@SiO_2 (0.5 g) was sonicated in dry toluene (5 ml) for 30 min. 3-(Triethoxysilyl)propylamine (1 mmol, 0.179 g) was added to the dispersed MNPs in toluene under nitrogen atmosphere. The resultant mixture was stirred under reflux conditions for 12 h under nitrogen atmosphere. Amino-functionalized core–shell structure was separated usinf an external magnet and washed with toluene (3 × 5 ml) in order to remove unreacted species and dried at 80 °C for 6 h.

3.4 | Preparation of Ligand-Functionalized Fe_3O_4@SiO_2

As shown in Scheme 1, the modification of Fe_3O_4@SiO_2-NH_2 was carried out via reaction between the amino group and 3-chloropropane-1,2-diol. Thus, 3-chloropropane-1,2-diol (1 mmol, 0.110 g) was added to a dispersed mixture of Fe_3O_4@SiO_2-NH_2 (0.5 g) in ethanol (20 ml). The resulting mixture was refluxed under inert atmosphere for 24 h. After completion, the product was separated using an external magnet, washed with ethanol and dried at 80 °C for 6 h.

3.5 | Preparation of Cu Immobilized on Fe_3O_4@SiO_2-Lig

Ligand-functionalized MNPs (0.1 g) were sonicated in toluene (20 ml) for 10 min. A solution of $Cu(OAc)_2$ (0.2 M) was added to the dispersed MNPs and the mixture was sonicated for 20 min. Then, the resulting mixture was stirred at 60 °C for 24 h. After completion, the catalyst was washed three times with water and ethanol to remove the unreacted salt and finally dried at 80 °C for 6 h.

3.6 | General Procedure for Synthesis of Aldoxime Derivatives

According to the literature,[31] $NH_2OH{\cdot}HCl$ (0.3 g, 4.3 mmol) was added to a stirred mixture of ZnO (0.16 g, 2 mmol) and aldehyde (1 mmol) at 80 °C in an oil bath. The progress of the reaction was monitored by TLC. After complete disappearance of the starting material, CH_2Cl_2 (20 ml) was added and washed with water (2 × 20 ml). The organic layer was dried (Na_2SO_4) and evaporated to afford the aldoxime.

3.7 | General Procedure for Synthesis of Amide Derivatives (1–20) Catalysed by Fe_3O_4@SiO_2-Lig-Cu MNPs

To a mixture of nanocatalyst (4 mol%) in PEG (0.50 ml), benzaldoxime (1.00 mmol, 0.121 g) was added with stirring. The reaction mixture was stirred at 80 °C for 1 h. After completion of the reaction, as indicated by TLC, the reaction mixture was diluted with water and the catalyst separated using an external magnet. Then the reaction mixture was extracted using ethyl acetate (3 × 5 ml). The organic layer was dried over anhydrous Na_2SO_4 and purified by crystallization from ethylacetate–hexane (1:2) to afford the products (**1**–**20**). All aromatic and heteroaromatic amides were previously reported and characterized using FT-IR spectroscopy and mass spectrometry (see supporting information) as well as comparison of their melting points with reported ones.[17–33] The structure of selected products (**14**, **16**, **19**, **20**) was further confirmed using ^{1}H NMR and ^{13}C NMR spectroscopy (see supporting information).

4 | CONCLUSIONS

In summary, a new heterogeneous catalyst (Fe_3O_4@SiO_2-Lig-Cu MNPs) was prepared. Various techniques such as FT-IR spectroscopy, XRD, SEM, EDX analysis, TEM, TGA, ICP analysis and VSM were applied in order to characterize the catalyst structure. According to XRD

and TEM results, average particle size of nanoparticles obtained was between approximately 20 and 25 nm. Catalytic activity of the newly synthesized catalyst was investigated in primary amide preparation through Beckmann rearrangement of aldoximes. Mild reaction conditions, using inexpensive reagents, high yields of products especially for heteroaromatic amides, short reaction times, easy work-up procedure, using PEG as a green reaction medium, reusability of the catalyst and compatibility with a wide range of functional groups in applied substrates are the main features of this approach which provides an efficient and eco-friendly process for the preparation of aromatic amides.

ACKNOWLEDGEMENT

The authors gratefully acknowledge the partial support of this study by Ferdowsi University of Mashhad Research Council (grant number 3/41331).

ORCID

Ali Shiri http://orcid.org/0000-0002-5736-6287
Hossein Eshghi http://orcid.org/0000-0002-8417-220X

REFERENCES

[1] L. T. Aany Sofia, A. Krishnan, M. Sankar, N. K. Kala Raj, P. Manikandan, P. R. Rajamohanan, T. G. Ajithkumar, *J. Phys. Chem. C* **2009**, *113*, 21114.

[2] Z.-L. Lu, E. Lindner, H. A. Mayer, *Chem. Rev.* **2002**, *102*, 3543.

[3] M. Kidwa, J. Arti, S. Bhardwaj, *Mol. Diversity* **2012**, *16*, 121.

[4] a) R. W. Murray, *Chem. Rev.* **2008**, *108*, 2688; b) R. M. Crooks, M. Q. Zhao, L. Sun, V. Chechik, L. K. Yeung, *Acc. Chem. Res.* **2001**, *34*, 181; c) P. K. Jain, K. S. Lee, I. H. El-Sayed, M. A. El-Sayed, *J. Phys. Chem. B* **2006**, *110*, 7238; d) S. Y. Han, Q. H. Guo, M. M. Xu, Y. X. Yuan, L. M. Shen, J. L. Yao, W. Liu, R. A. Gu, *J. Colloid Interface Sci.* **2012**, *378*, 51.

[5] a) D. P. He, C. Zeng, C. Xu, N. C. Cheng, H. G. Li, S. C. Mu, M. Pan, *Langmuir* **2011**, *27*, 5582; b) X. J. Bian, X. F. Lu, E. Jin, L. R. Kong, W. J. Zhang, C. Wang, *Talanta* **2010**, *81*, 813; c) M. Kim, J. C. Park, A. Kim, K. H. Park, H. Song, *Langmuir* **2012**, *28*, 6441.

[6] a) H. Q. Wang, X. Wei, K. X. Wang, J. S. Chen, *Dalton Trans.* **2012**, *41*, 3204; b) H. F. Wang, H. Ariga, R. Dowler, M. Sterrer, H. J. Freund, *J. Catal.* **2012**, *286*, 1; c) W. Ludwig, A. Savara, B. Brandt, S. Schauermann, *Phys. Chem. Chem. Phys.* **2011**, *13*, 966; d) B. Maleki, H. Eshghi, M. Barghamadi, N. Nasiri, A. Khojastehnezhad, S. S. Ashrafi, O. Pourshiani, *Res. Chem. Int.* **2016**, *42*, 3071; e) B. Maleki, B. S. Barat Nam Chalaki, S. S. Ashrafi, E. Rezaee Seresht, F. Moeinpour, A. Khojastehnezhad, R. Tayebee, *App. Organometal. Chem* **2015**, *29*, 290; f) B. Maleki, E. Sheikh, E. Rezaee Seresht, H. Eshghi, S. S. Ashrafi, A. Khojastehnezhad, H. Veisi, *Org. Prep. Proced. Int.* **2016**, *48*, 37.

[7] a) J. M. Humphrey, A. R. Chamberlin, *Chem. Rev.* **1997**, *97*, 2243; b) T. Cupido, J. Tulla-Puche, J. Spengler, F. Albericio, *Curr. Opin. Drug Discov. Dev.* **2007**, *10*, 768; c) V. R. Pattabiraman, J. W. Bode, *Nature* **2011**, *480*, 471; d) C. L. Allen, J. M. J. Williams, *Chem. Soc. Rev.* **2011**, *40*, 3405.

[8] M. I. Hegab, A.-S. M. Abdel-Fattah, N. M. Yousef, *Pharmazie Chem. Life Sci.* **2007**, *340*, 396.

[9] N. Siddiqui, M. S. Alam, W. Ahsan, *Acta Pharm.* **2008**, *58*, 445.

[10] K. Galewicz-Walesa, A. Pachuta-Stec, *Med. Acad. Lublin* **2003**, *9*, 118.

[11] T. L. Graybill, M. J. Ross, B. R. Gauvin, J. S. Gregory, A. L. Harris, M. A. Ator, J. M. Rinker, R. E. Dolle, *Bioorg. Med. Chem. Lett.* **1992**, *1375*.

[12] A. Warnecke, I. Fichtner, G. Sab, F. Kratz, *Pharmazie Chem. Life Sci.* **2007**, *340*, 8.

[13] a) C. A. G. N. Montalbetti, V. Falque, *Tetrahedron* **2005**, *61*, 10827; b) E. Valeur, M. Bradley, *Chem. Soc. Rev.* **2009**, *38*, 606.

[14] a) J. S. Carey, D. Laffan, C. Thomson, M. T. Williams, *Org. Biomol. Chem.* **2006**, *4*, 2337; b) D. J. C. Constable, P. J. Dunn, J. D. Hayler, G. R. Humphrey, J. L. Leazer Jr., R. J. Linderman, K. Lorenz, J. Manley, B. A. Pearlman, A. Wells, A. Zaks, T. Y. Zhang, *Green Chem.* **2007**, *9*, 411.

[15] a) C. L. Allen, J. M. J. Williams, *Chem. Soc. Rev.* **2011**, *40*, 3405; b) V. R. Pattabiraman, J. W. Bode, *Nature* **2011**, *480*, 471; c) S. Roy, S. Roy, G. W. Gribble, *Tetrahedron* **2012**, *68*, 9867; d) P. Crochet, V. Cadierno, *Chem. Commun.* **2015**, *51*, 2495.

[16] S. K. Sharama, S. D. Bishopp, C. L. Allen, R. Lawrence, M. J. Bamford, A. A. Lapkin, P. Plucinski, R. J. Watson, J. M. J. Williams, *Tetrahedron Lett.* **2011**, *52*, 4252.

[17] Y. M. Liu, L. He, M. M. Wang, Y. Cao, H. Y. He, K. N. Fan, *ChemSusChem* **2012**, *5*, 1392.

[18] X. Wu, H. Neumann, M. Beller, *Chem. Eur. J.* **2012**, *18*, 419.

[19] P. J. Gonzalez-Liste, V. Cadierno, S. E. Garcia-Garrido, *ACS Sustainable Chem. Eng* **2015**, *3*, 3004.

[20] R. G. Álvarez, M. Zablocka, P. Crochet, C. Duhayon, J.-P. Majoral, V. Cadierno, *Green Chem.* **2013**, *15*, 2447.

[21] R. G. Álvarez, A. E. D. Alvarez, P. Crochet, V. Cadierno, *RSC Adv.* **2013**, *3*, 5889.

[22] N. C. Ganguly, S. Roy, P. Mondal, *Tetrahedron Lett.* **2012**, *53*, 1413.

[23] A. Mishra, A. Ali, S. Upreti, R. Gupta, *Inorg. Chem.* **2008**, *47*, 154.

[24] D. Antoniak, A. Sakowicz, R. Loska, M. Mąkosza, *Synlett* **2015**, *26*, 84.

[25] H. Sharghi, M. Hosseini Sarvari, *Tetrahedron* **2002**, *58*, 10323.

[26] M. A. Schade, G. Manolikakes, P. Knochel, *Org. Lett.* **2010**, *12*, 3648.

[27] S. Park, Y. Choi, H. Han, S. H. Yang, S. Chang, *Chem. Commun.* **1936**, *2003*.

[28] S. C. Ghosh, J. S. Y. Ngiam, A. M. Seayad, D. T. Tuan, C. L. L. Chai, A. Chen, *J. Org. Chem.* **2012**, *77*, 8007.

[29] Y. Ito, H. Yoshikatsu, S. Ohba, *Tetrahedron* **2000**, *56*, 6833.

[30] N. Ambreen, T. Wirth, *Eur. J. Org. Chem.* **2014**, *7590*.

[31] H. Sharghi, M. Hosseini, *Synthesis*, **2002** 1057.

[32] S. Rostamnia, N. Nouruzi, H. Xin, R. Luque, *Catal. Sci. Technol.* **2015**, *5*, 199.

[33] J. Mauger, T. Nagasawa, H. Yamada, *Tetrahedron* **1989**, *45*, 1347.

[34] a) J. S. Lee, E. J. Lee, H. J. Hwang, *Trans. Nonferrous Met. Soc. China* **2012**, *22*, 702; b) J. G. Shao, X. C. Xie, Y. J. Xi, X. N. Liu, Y. X. Yang, *Glass Phys. Chem.* **2013**, *39*, 329.

[35] M. Rajabzadeh, H. Eshghi, R. Khalifeh, M. Bakavoli, *RSC Adv.* **2016**, *6*, 19331.

[36] M. Esmaeilpour, J. Javidi, F. Nowroozi Dodeji, M. Mokhtari Abarghoui, *J. Mol. Catal. A* **2014**, *393*, 18.

[37] a) G. Lucovsky, J. Yang, S. S. Chao, J. E. Tyler, W. Czubatyj, *Phys. Rev. B* **1983**, *28*, 3225; b) R. Jahanshahi, B. Akhlaghinia, *RSC Adv.* **2016**, *6*, 29210.

[38] D. J. Quesnel, D. S. Rimai, L. H. Sharpe, *Particle Adhesion: Applications and Advances*, Taylor and Francis **1998**.

[39] L. Zhou, C. Gao, W. Xu, *Langmuir* **2010**, *26*, 11217.

[40] G. Lucovsky, J. Yang, S. S. Chao, J. E. Tyler, W. Czubatyj, *Phys. Rev. B* **1983**, *28*, 3225.

[41] L. Xiaojuan, J. Guoyuan, Z. Liping, Y. Yuxiang, L. Xiangnong, *Glass Phys. Chem.* **2011**, *37*, 459.

[42] J. V. Bellini, R. Machado, M. R. Morelli, R. H. G. A. Kiminami, *Mater. Res.* **2002**, *5*, 453.

[43] R. M. Magdalene, E. G. Leelamani, G. N. M. Nanje, *J. Mol. Catal. A* **2004**, *17*, 223.

[44] M. A. Ghasemzadeh, M. H. Abdollahi-Basir, M. Babaei, *Green Chem. Lett. Rev.* **2015**, *8*, 40.

SUPPORTING INFORMATION

Additional Supporting Information may be found online in the supporting information tab for this article.

How to cite this article: Keyhaniyan M, Shiri A, Eshghi H, Khojastehnezhad A. Novel design of recyclable copper(II) complex supported on magnetic nanoparticles as active catalyst for Beckmann rearrangement in poly(ethylene glycol). *Appl Organometal Chem*. 2018;e4344. https://doi.org/10.1002/aoc.4344